Inorganica Chimica Acta 369 (2011) 62–70

Contents lists available at ScienceDirect

Inorganica Chimica Acta

journal homepage: www.elsevier.com/locate/ica

Measurement of the barrier to inversion of configuration in acyclic phosphite triesters

Joshua A. Mukhlall, William H. Hersh *

Department of Chemistry and Biochemistry, Queens College and the Graduate Center of the City University of New York, Flushing, NY 11367-1597, United States

ARTICLE INFO

Article history:
Available online 21 November 2010

Dedicated to Robert G. Bergman

Keywords:
Phosphite epimerization
Chiral phosphites
Inversion
Kinetics
Oligonucleotides

ABSTRACT

Synthesis of three acyclic chiral phosphites is reported, in the form of dithymidine phosphite triesters. These diastereomerically pure P-stereogenic phosphites undergo epimerization at a measurable rate at 150 °C. When the alcohols on the deoxyribose moieties are protected as acyls, decomposition is minimized and by computer fitting, rate constants for epimerization can be extracted. These allow for the first time calculation of the barrier to inversion of configuration in phosphite triesters, giving $\Delta G^{\dagger}(150\ ^{\circ}C) = 33.0 \pm 0.2$ kcal mol^{-1}, comparable to the inversion barrier seen for phosphines.

1. Introduction

In a paper published 40 years ago, Mislow showed that the epimerization of chiral phosphines takes place at measurable rates at 130 °C with inversion barriers of 29–36 kcal mol^{-1} [1]. No similar reports exist for acyclic chiral phosphites, and in fact we are aware of only one report of isolation of P-epimers of acyclic P-stereogenic phosphites [2]. Given the interest in chiral phosphites and related species in asymmetric hydrogenation [3–5] and hydroformylation [6–11] – albeit, not for P-stereogenic phosphites – we sought to establish whether or not P-stereogenic phosphites would undergo inversion at phosphorus.

Numerous hints may be found in the literature that acyclic phosphites are configurationally stable at room temperature. For instance, the Just [12,13], Agrawal [14–16], Beaucage [17], and Wada [18–20] research groups have reported syntheses of P-stereogenic dinucleoside phosphorothioates by routes that generate a phosphite triester that was not isolated but instead was characterized only by ^{31}P NMR [21] or in most cases immediately sulfurized to give a phosphite sulfide [12–20]. A representative example, due to Beaucage and coworkers [17], is shown in Scheme 1a, where coupling of P-stereogenic phosphoramidite **1** with 3′-protected nucleoside **2** gave the intermediate phosphite triester **3**; this was immediately sulfurized to give the phosphite sulfide **4** as a single diastereomer.

A similar example was reported by Hata (Scheme 1b), which differs in that each of the reactions that generated and consumed the intermediate phosphite triester took place over the course of 1 h. That is, alkoxycarbonyl phosphonate **5**, which was separated from its P-epimeric diastereomer by preparative HPLC [22,23], was converted to phosphite triester **6** over a period of 1 h and was then treated *in situ* with sulfur for another 1 h followed by hydrolysis of the silyl group to give **7** in high diastereomeric purity.

The first clear-cut example of configurational stability of a phosphite triester was Makino's report (Scheme 1c) that selected phosphite triesters could be chromatographically separated to give ~100 mg quantities of S_P and R_P-**9** starting from phosphoramidite **8** [2,24]. Characterization consisted only of elemental analysis of the mixture and ^{1}H and ^{31}P NMR spectra of the individual diastereomers, and did not include any discussion of diastereomeric purity of the ~100 mg quantities. A 20 mg sample with a diastereomeric purity of 97.1%, apparently determined by HPLC, underwent substitution by 2-methyl-1-propanol to give phosphite triester **10a** which was determined to be 94% diastereomerically pure on the basis of ^{31}P NMR, although it was not further characterized. Substitution of the phenol moieties in S_P and R_P-**9** by a 3′-protected nucleoside gave phosphite triester **10b** in moderate to good yields but with only moderate stereoselectivities (on the basis of ^{31}P NMR), but further characterization of this dinucleoside phosphite triester was not reported. Nevertheless, this report is the only one of which we are aware to describe isolation of acyclic P-stereogenic phosphites, and certainly suggests them to have configurational stability at room temperature.

There are a few examples in the literature of apparent inversion of *cyclic* phosphites (Scheme 2). In the first example (Scheme 2a), Bentrude reported that the 3′, 5′-cyclic thymidine phosphite triester, initially formed as a 40:60 mixture of isomers **11-ax:11-eq**,

* Corresponding author. Tel.: +1 718 9974144; fax: +1 718 9975531.
E-mail address: william.hersh@qc.cuny.edu (W.H. Hersh).

0020-1693/$ - see front matter © 2010 Elsevier B.V. All rights reserved.
doi:10.1016/j.ica.2010.11.022

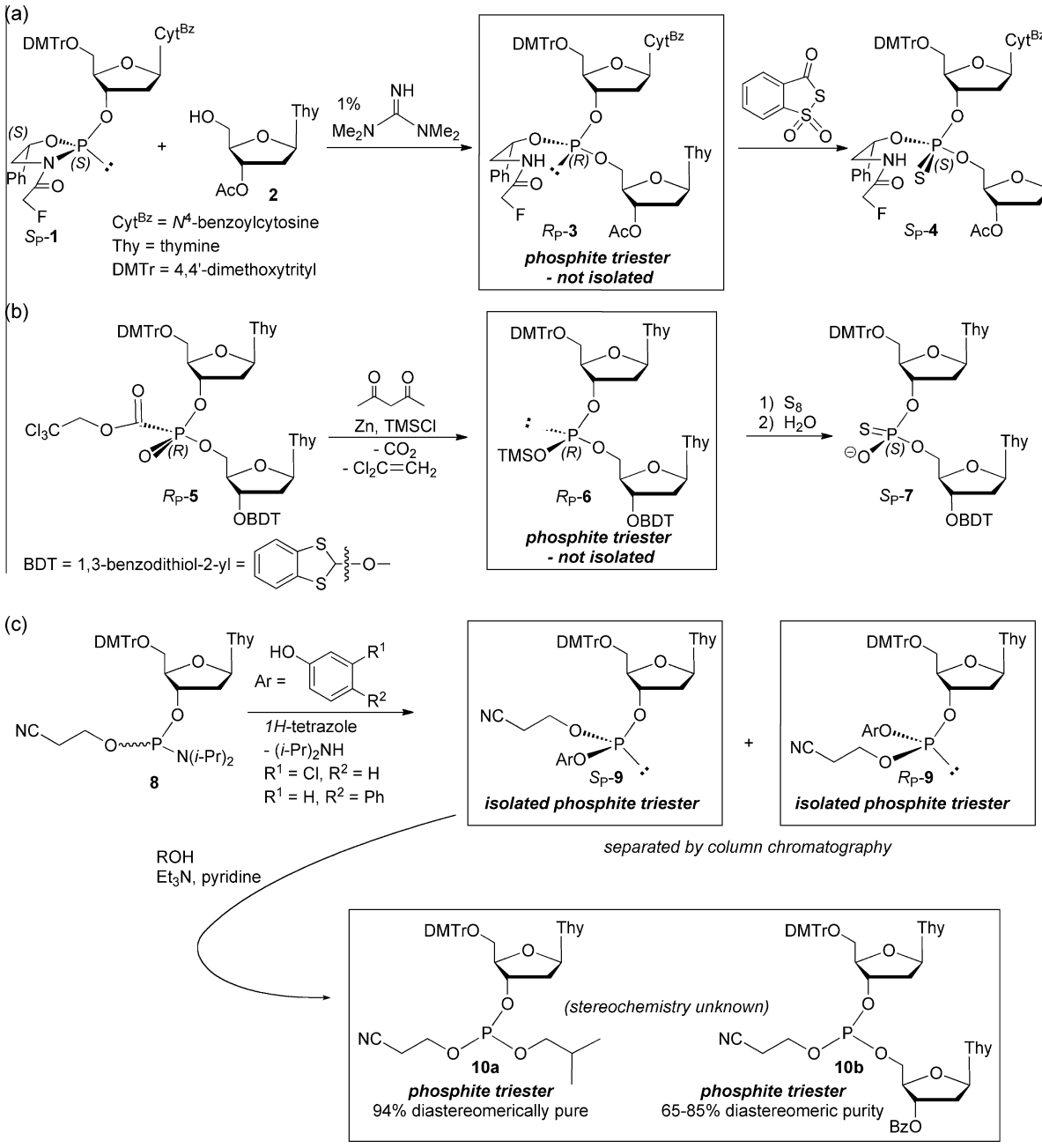

Scheme 1. Acyclic P-stereogenic phosphite triesters.

isomerized to a 95:5 mixture by heating for 30 min at ~60 °C in the presence of pyridinium chloride [25]. Hayakawa reported that a similar cyclic thymidine phosphite triester isomerized from a 50:50 mixture of isomers **12-ax**:**12-eq** to give **12-ax** exclusively by heating at 55 °C for 36 h in the presence of *1H*-tetrazole (Scheme 2b) [26]. The thermodynamic preference for P-axial isomers in six-membered rings (while maintaining the thermodynamic preference for equatorial substituents on the carbon atoms) is well-known [27], so both **11** and **12** provide further examples of this. In the last example (Scheme 3c), Gordillo measured the rates of isomerization of *cis*-**13** to *trans*-**13** at temperatures from 50 to 75 °C and calculated $\Delta G^{\dagger} = 26.9 \pm 1.0$ kcal mol^{-1} for the process [28]. In fact, the reaction is likely to be induced just like the isomerizations of **11** and **12**, since the *cis*-**13** was not separated from the Et_3NH^+ Cl^- formed during its synthesis, and the isomerization proceeded at a reasonable rate at 60 °C, not unlike that seen for **11** with pyridinium chloride and **12** with tetrazole.

While not strictly related to these examples, one of the best-known examples of isomerization of a five-membered ring phosphorus heterocycle is that of ephedrine-derived **14** (Scheme 3). When the reaction was carried out by mixing ephedrine with $PhP(NEt_2)_2$ at 105 °C overnight, the pure *trans*-diastereomer was obtained [29], but Brown showed that mixing ephedrine with $PhPCl_2$ at 0 °C gave a 1:1 mixture of *cis*:*trans* diastereomers. Like the phosphite triesters **11**–**13**, this mixture – in the presence of the ammonium salt that formed during the reaction – isomerized over 18 h at rt to give the pure *trans*-diastereomer [30].

The question these examples raise is whether or not the apparent phosphite epimerization in **11**–**14** is due to phosphorus inversion, or rather to a ring opening/ring closing type of inversion that would not be available to an acyclic phosphite without scrambling of alkoxy substituents. That exact scenario has in fact been observed for H-phosphonate "epimerization" in the presence of base, where the apparent inversion was accompanied by alkoxy

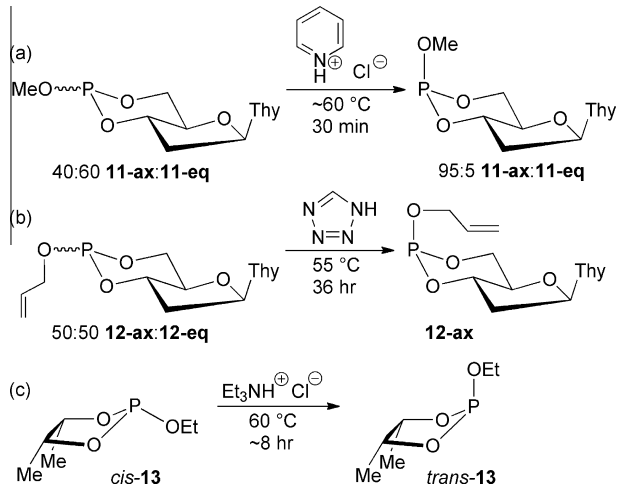

Scheme 2. Epimerization in cyclic phosphite triesters.

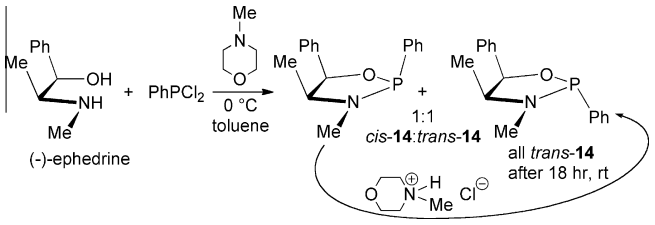

Scheme 3. Epimerization of an ephedrine-derived heterocycle.

scrambling and so was clearly due to a bond-cleavage process [31,32]. If isomerization of the cyclic phosphites were occurring by inversion, we would expect the barrier to be raised due to angle strain in the ring at the planar transition state, and so inversion of an acyclic phosphite would be expected to occur more readily. On the other hand, if isomerization of **11**–**14** were occurring by a ring-opening/ring-closing mechanism, we would expect inversion of an acyclic phosphite to perhaps be more comparable to that of a chiral phosphine.

In this paper, we report (1) the synthesis and characterization of epimeric acyclic dinucleoside trialkoxy phosphite esters, (2) protecting group conversions to give phosphite triesters that are relatively stable at 150 °C, (3) rates of epimerization at 150 °C that are due to phosphorus inversion and (4) attempts to raise the rate of epimerization using acidic and radical reagents. These results provide the first measure of the barrier to phosphite triester inversion.

2. Results and discussion

2.1. Synthesis of epimeric phosphite triesters

While Makino had reported the synthesis of triesters **10a**,**b** (Scheme 1), we wanted a method that would be suitable for both larger amounts of material and higher purity. The synthesis and separation of the P-epimers of a dithymidine boranophosphate triester that had been reported by Just and coworkers appeared to be just such a better option [33], and so this approach coupled with deboronation was taken to isolate the two desired P-epimers. The requisite mixture of diastereomeric phosphite triesters **15** (Scheme 4) was synthesized in high yield using minor modifications of literature methods [33–37], except that for the final coupling step of the phosphoramidite and the 3′-protected thymidine, we found that use of a 2:1 mixture of pyridinium trifluoroacetate/*N*-methylimidazole (PTFA/NMI) as the activator [38] was superior to other procedures such as using tetrazole [33]. Before proceeding to the boronation step, we attempted to directly separate the diastereomers of **15**. However, no solvent system was found to give any separation on TLC, and attempts to split the eluting band in fractions by column chromatography also failed.

Just reported that the boronation of the phosphite triester **15** with $Me_2S{\cdot}BH_3$ also resulted in removal of the DMTr group, which had to be reinstalled before the separation of the diastereomers could be accomplished [33]. Since the reaction of BH_3 with the phosphite was reported to occur "within 5–10 min," we tried both a short reaction time and rapid work-up. In fact, we found that carrying out the reaction at 0 °C for 15 min and then quickly passing the reaction solution through a pad of silica gel with the aid of THF, allowed for phosphite boronation without deprotection of the DMTr group, in 95% yield (Scheme 4). The diastereomers of boranophosphate **16** were then separated by silica gel column chromatography as reported, to give a 25% yield of S_P-**16** and 23% yield of R_P-**16**, each on the basis of the total amount of **16**. Deprotection was accomplished by addition of 10 equivalents of DABCO to S_P-**16** at rt for 37 h. TLC of the reaction solution showed movement of the product with the solvent front (THF) and some UV active material at the origin of the plate. After passing the crude material through a pad of silica gel, a 60% yield of S_P-**15** was obtained. This low yield might be due to the conversion of tetravalent boranophosphate **16** to a pentavalent boranophosphate species due to elimination of the β-cyanoethyl group by DABCO, but no attempt was made to optimize this reaction.

As will be made clear below, S_P-**15** was not a suitable candidate for the study of phosphite inversion, and the next compound to be selected was the unprotected dithymidine triester. The DMTr group was removed with 2% $CHCl_2COOH/CH_2Cl_2$ over 20 min to give compounds S_P-**17** and R_P-**17** from S_P and R_P-**16**, respectively, in approximately 80% yields. For the deprotection of the TBDMS group, Just and coworkers used TBAF (1 eq)/AcOH (24 eq) in THF, but we found that this mixture resulted in a very slow deprotection with decomposition of the compound over the reaction time. Using TBAF without the acetic acid caused extensive decomposition to unknown compounds as indicated by TLC; one possible side reaction might be a β-cyanoethyl elimination. HF·Et_3N and HF·pyridine were tried next, and while HF·Et_3N resulted in slow deprotection with some decomposition of the compound (observed by TLC), the latter reagent was found to be much more efficient in the deprotection of the TBDMS group, giving yields of 87% and 85% for S_P-**18** and R_P-**18**, respectively. Removal of the BH_3 group from S_P-**18** and R_P-**18** was accomplished by reaction with a large excess of pyridine (130 eq) which gave superior results to that from the reaction of DABCO with **16**: in this case, 90% yields of S_P-**19** and 80% of R_P-**19** were obtained after purification by silica gel chromatography.

Once again, as will be seen below, **19** turned out not to be a suitable candidate for epimerization, and so the diacyl analogue was synthesized by reaction of **18** with acetic anhydride in pyridine. After 24 h of stirring at rt, complete acetylation of the two hydroxyl groups together with the expected removal of the BH_3 group was achieved in one step to afford diacyldinucleosides S_P-**20** and R_P-**20**, which were purified by flash chromatography under nitrogen to give >80% yield of each compound.

2.2. Attempted epimerization of 15 and 19

A sample of the phosphite triester S_P-**15** dissolved in approximately 0.5 mL toluene-d_8 was sealed in an NMR tube under vacuum, and then heated at 150 °C in an oil bath. After ~7 h of

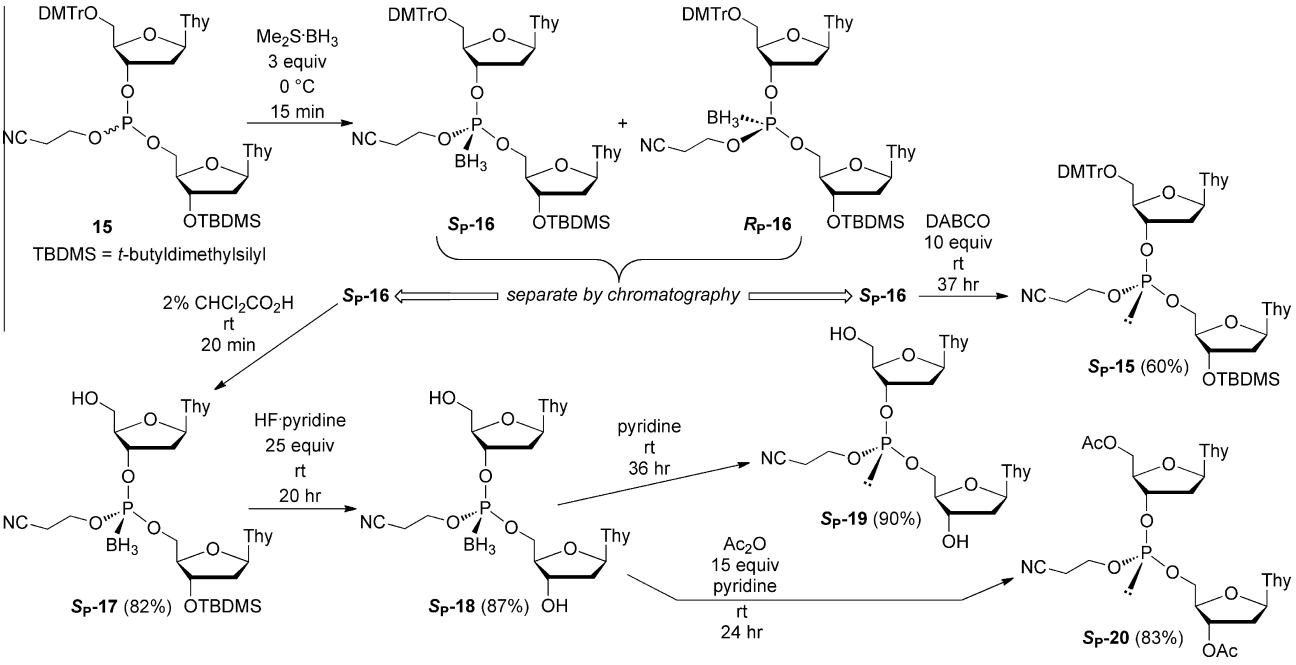

Scheme 4. Separation of S_P and R_P-**16** and conversion to P-stereogenic phosphite triesters.

heating, the ^{31}P NMR spectrum of the sample exhibited ~2.7% decomposition to an unknown species at ~27 ppm, and two peaks at 139.38 and 138.75 ppm corresponding to the two diastereomers of compound **15**. However, the extent of epimerization (4.7% calculated as [R_P-**15**/(S_P-**15** + R_P-**15**)]) was not much greater than the extent of decomposition, and longer periods of heating the sample only resulted in extensive decomposition of the phosphite triester without comparable epimerization.

Epimerization of the deprotected diol triester **19** was examined next, on the basis of the hypothesis that the decomposition might be due to the elimination of the DMTr and/or TBDMS groups at 150 °C. Samples of S_P-**19** and R_P-**19** were dissolved in CD_3CN (the diols gave sharper spectra in acetonitrile than in toluene), sealed in NMR tubes, and placed in an oil bath maintained at 150 ± 0.2 °C. After heating the solution of S_P-**19** for 1 h, the ^{31}P NMR spectrum of the solution exhibited peaks at 140.78 and 140.31 ppm corresponding to S_P-**19** and R_P-**19**, respectively, and peaks at 140.67 and 140.13 ppm corresponding to ~2.3% decomposition. The extent of inversion calculated as above was found to be 24%. While this was a significant improvement and also suggested faster epimerization in acetonitrile than in toluene, longer periods of heating again resulted in decomposition of the phosphite triester to unknown species with chemical shifts close to those of the diol phosphite triesters, most likely due to cyclization of either one of the thymidine residues with simultaneous elimination of 2-cyanoethanol. This side reaction made monitoring of the inversion difficult because the ^{31}P NMR peaks of the two diastereomers of phosphite triester **19** and the unknown species were too close to be integrated with accuracy.

2.3. Epimerization of diacyls S_P-20 and R_P-20

Since it was clear that heating the diol would not allow the rate of epimerization to be measured, the alcohols were next reprotected to give the diacyl **20**, which we hypothesized would have sufficient thermal stability. This proved to be successful, since while phosphite decomposition still occurred, it did not prevent epimerization from proceeding to equilibrium from both P-epimers. A total of six experiments were carried out (see Section 4 and Supplementary material for details), each in pairs of two in order to compare the inversions of S_P-**20** and R_P-**20**. One pair (exp. 1–2) was carried out with Ph_3P as an internal standard, while two pairs (exp. 3–6) were carried out with Ph_3P as an external standard in acetonitrile solution in a sealed capillary tube; for one of the external standard pairs (exp. 5–6), all glassware contacted by the phosphites was silanized with Me_2SiCl_2 [39]. All reactions were run in a thermostatted oil bath at 150 ± 0.2 °C in sealed NMR tubes; once again CD_3CN was used as the solvent since it gave rise to spectra with sharper peaks than when toluene-d_8 was used.

Examination of plots of concentration versus time showed that equilibration occurred within about 3 h, after which the concentrations declined slowly or leveled off. Examination of the total phosphite concentration versus time made it clear that decomposition was relatively rapid during the first ~2 h and slowed down after that. It was also clear that standard kinetic plots would not suffice to separate the epimerization from decomposition. We had previously developed a computer program, *CRK2005* (for Complex Reaction Kinetics) [40], that allows one to fit rate constants to observed data in multiple kinetic runs for any set of coupled differential equations. A number of kinetic mechanisms of decomposition were considered before one was found that allowed a good fit to the observed kinetic data. These are described in detail now.

2.4. Rate of phosphite decomposition using computer modeling

We started by using the data from the silanized runs, which gave the smoothest results, and were virtually superimposable for the two runs starting from the same concentrations of S_P-**20** and R_P-**20**, respectively. In order to model phosphite decomposition, we followed total concentration of the two epimers versus time, before adding in the complication of epimerization. As shown in Fig. 1a, the reaction of S_P-**20** was followed for 8 h (i.e., 28 800 s) while R_P-**20**was followed only for 4 h (14 400 s). Simple first order decomposition of the phosphites gave a poor fit to the observed data points, and second order decomposition (for which we had no rational mechanism) gave only a marginally better fit, as seen; the kinetic schemes considered are shown in Fig. 2, which includes the epimerization steps. The numerical results are collected in Table 1, which lists the reduced chi squared function χ^2_v and a more intuitive % error per data point, both of which have been defined

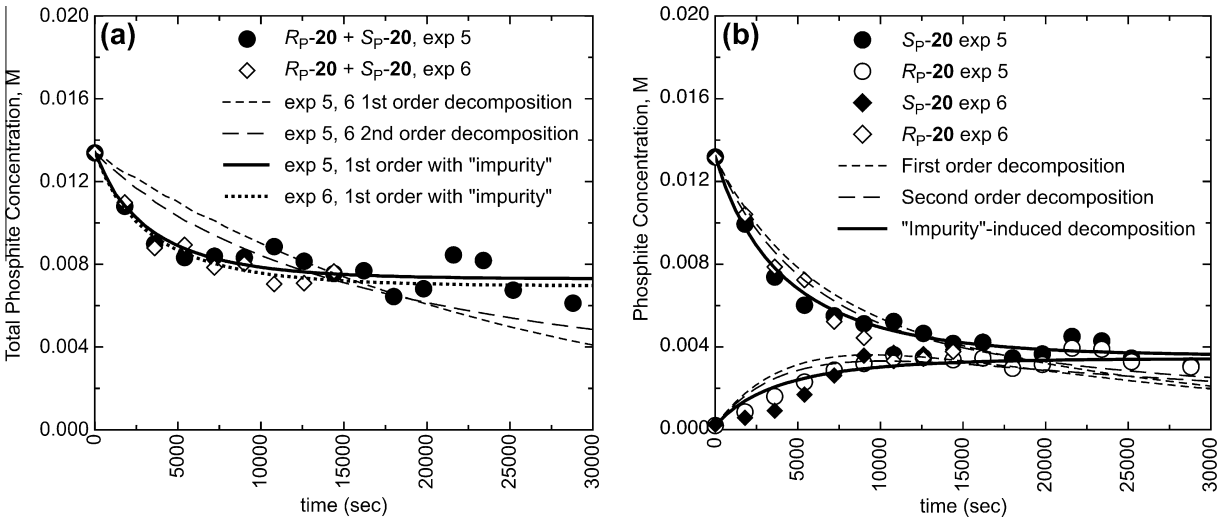

Fig. 1. Plots of total phosphite concentration (a), [R_P-**20**] + [S_P-**20**], and phosphite epimerization (b), starting from S_P-**20** (exp. 5) and R_P-**20** (exp. 6), determined by ^{31}P NMR integration vs. an external standard (PPh_3 in CH_3CN solution in a sealed capillary tube) vs. time at 150 °C. The calculated best-fit lines for each of three mechanisms discussed in the text (Fig. 2) are shown.

previously [40], and both of which analytically bear out the above visual conclusion that the second order mechanism is slightly better. Clearly both sets of calculated data showed that any mechanism that required the phosphite concentrations to approach zero in first or second order fashion would not fit the observed data, in which the phosphite concentrations decay very slowly or level out. One can imagine some adventitious species that might react with the phosphites resulting in decomposition, but after that species is consumed, the decomposition would end. In order to model this, *CRK2005* allows the concentration of any initial species to be varied, within limits, to give the best fit, since the numerical integration method for calculating the outcomes of coupled rate equations depends on the values of the initial starting points. This was done by allowing the concentration of an initial "impurity" to vary, along with the second order rate constant, and as seen this gave an excellent fit to the data, both visually and (Table 1) analytically. Similarly, all six runs could be fit to this mechanism, and while the overall fit is not as good (χ^2_v and % error of 2.4% and 9.4%, respectively, compared to 1.5% and 6.8% for experiments 5–6 alone; see Supplementary material for the six plots), the fact that six runs can be fit to the same rate constant (and comparable "impurity" concentrations) lends confidence that the mechanism is reasonable. It should be noted that, not surprisingly, multiple sets of decomposition rate constant k_3 and impurity concentrations give comparable fits to individual runs (as seen for experiments 5 and 6), but when all runs are considered simultaneously it is less likely that more than one set will fit. The required impurity concentrations in order for the silanized experiments to fit is actually higher, a counterintuitive result, but while the data is smoother, the extent of decomposition was also clearly greater in those two experiments.

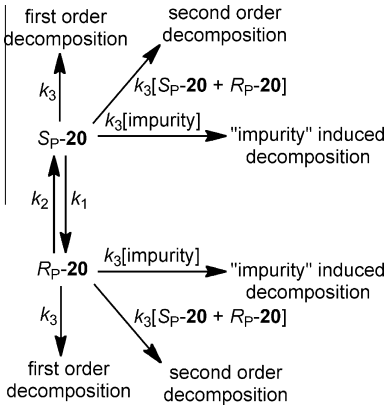

Fig. 2. Proposed kinetic scheme for equilibration and decomposition of S_P-**20** and R_P-**20**; only one of the three k_3 mechanisms would be operative.

2.5. Rate of phosphite epimerization using computer modeling

As before, the two silanized runs were considered first. The kinetic pathways to be fit are shown above in Fig. 2; even though we found that the "impurity" mechanism was best, it seemed reasonable to check how much the best fit rate constants for epimerization would vary with the decomposition pathway chosen. As seen in Fig. 1b, the best-fit lines for the first and second-order decomposition mechanisms are very similar (for simplicity only the fit for run 5 is shown, but that for run 6 is nearly coincident). However, once again the fit for the "impurity" mechanism is seen to be significantly better, and as seen in Table 1, the analytical error estimates (χ^2_v and % error) are much better.

Fitting the epimerization and decomposition rates to all six runs yields rate constants that are only slightly different (Table 1; graphs and data may be found in the Supplementary material). The fact that all the data can be simultaneously fit provides strong support for the calculated rate constants.

In closing this section, we note one final complication. In several of the experiments, formation of the minor isomer started more slowly than calculated by the "impurity" mechanism (or both of the others), which might be accounted for by an imperfect match of the decomposition mechanism. This can be seen for formation of S_P-**20** in experiment 6 in Fig. 1b, and to a much lesser extent for R_P-**20** in experiment 5. That is, the epimerization appears autocatalytic, as if some impurity was generated during the reaction that sped up epimerization. It was in fact for this reason that we silanized the glassware for experiments 5 and 6. While we could not find a mechanism that fit the data better, even if there was some autocatalytic component, our calculated epimerization rates k_1 and k_2 still represent *upper* limits for the rate of phosphite inversion. However, the epimerization of the major isomer for both experiments 5 and 6 did *not* start out slowly, so we suggest the apparent autocatalysis is most likely an artifact of experimental error in measurement of the small concentrations of the minor isomers.

Table 1
Calculated error estimates and best-fit rate constants for epimerization and decomposition of S_P-**20** and R_P-**20**[a] for the fit for the three mechanisms and six experiments, using *CRK2005*.

Experiment[b]	χ^2_v	% Error	k_1 (s^{-1})	k_2 (s^{-1})	k_3 (s^{-1} M^{-n}, n = 0,1)	[Impurity]
5, 6: 1st order decomposition	11.2	19.3			3.95 ± 0.19 E−5	
5, 6: 2nd order decomposition	6.9	15.1			4.93 ± 0.21 E−3	
5, 6: "impurity" decomposition	1.5	6.8			2.55 ± 0.13 E−2	0.00608 M
						0.00642 M
5, 6: 1st order decomposition	3.3	20.7	8.36 ± 0.45 E−5	8.86 ± 0.48 E−5	3.95 ± 0.20 E−5	
5, 6: 2nd order decomposition	2.2	16.9	7.92 ± 0.37 E−5	8.42 ± 0.39 E−5	4.36 ± 0.23 E−3	
5, 6: "impurity" decomposition	1.1	11.8	7.16 ± 0.23 E−5	7.46 ± 0.26 E−5	1.95 ± 0.13 E−2	0.00637 M
						0.00681 M
1–6: "impurity" decomposition	2.4	9.4			7.79 ± 0.50 E−3	*
1–6: "impurity" decomposition	1.5	16.9	6.73 ± 0.29 E−5	6.89 ± 0.31 E−5	1.29 ± 0.13 E−2	**

* For exp. 1–6, [impurity] = 0.00484, 0.00390, 0.00442, 0.00433, 0.00844, and 0.0113 M.
** For epimerization exp. 1–6, [impurity] = 0.00390, 0.00422, 0.00400, 0.00348, 0.00711, and 0.00833 M.
[a] See Ref. [40] for definitions of χ^2_v and % error, and text for the mechanisms and definitions of rate constants k_1–k_3.
[b] Data were fit to the decomposition rate alone using the sum [R_P-**20**] + [S_P-**20**] (only k_3) or to the epimerization and decomposition rate constants k_1–k_3 together.

2.6. Calculated inversion barrier

The critical result of the above fitting procedures is not the precise value of the epimerization or decomposition rate constants, but rather the derived value of the activation barrier for phosphite inversion. The best estimates for the epimerization rates, those obtained from all six runs in Table 1, gave the lowest rate constants, while the calculated results for the two silanized runs assuming first-order phosphite decomposition gave the highest values. Using these values and their deviations as the extremes gives an inversion barrier $\Delta G^{\dagger}$ = 33.0 ± 0.2 kcal mol^{-1}. The modest deviations in the individual rate constants have virtually no effect on $\Delta G^{\dagger}$, giving deviations of ±0.05 kcal mol^{-1}. We conclude, somewhat surprisingly, that the details of the decomposition pathways in fact really have no impact on the calculated inversion barrier.

2.7. Attempts to induce low temperature epimerization

Given the role posited for impurities in phosphite decomposition in the above kinetic scheme, it seemed reasonable to look at the role of potential impurities on epimerization. That is, there is a report in the literature of phosphine epimerization induced by I_2 [41], there are many reports of phosphite epimerization by ammonium salts and tetrazole as noted in Schemes 2 and 3, similar epimerization of chlorophosphines by acids and chlorides is known [18,42,43], and epimerization of phosphoramidites by tetrazole is well-documented [21,44]. Oxidation (as suggested by I_2) might be induced by a single-electron oxidizing reagent, for instance as seen in cation radical induced Diels–Alder reactions [45]; such a reagent might remove one of the lone pair electrons from the phosphorus atom and lower the inversion barrier, because this is the orbital that is likely to rise in energy during inversion. For these reasons, a variety of reagents were examined for induction of epimerization. Iodine immediately reacted with the model compound $(EtO)_3P$, apparently to give EtI via an Arbuzov reaction, and so the chiral phosphites were not tested. Radical reagents [45] galvinoxyl and $(BrC_6H_4)_3N^+$ $SbCl_6^-$ when combined with S_P-**15** gave decomposition but no inversion, and 1*H*-tetrazole, Et_3NH^+ Cl^-, $Me_2(NCCH_2)NH^+$ Cl^- [18], $MePh_2PH^+$ Cl^-, pyridinium chloride, and N-methylimidazolium chloride [46] similarly gave no inversion and in many cases also led to decomposition; details may be found in Supplementary material.

3. Conclusions

Unlike Mislow's study of phosphine inversion, where first order phosphine racemization was observed without detectable decomposition, the dinucleoside phosphite triesters used in the present study did undergo decomposition. However, the use of acyl protecting groups on the deoxyribose ring minimized the decomposition pathways, and allowed epimerization to be observed from both P-epimers. The rates of epimerization were similar from both diastereomers, and good fits of the data to first order epimerization coupled with an "impurity" induced decomposition pathway were found. Rate constants for epimerization, regardless of the decomposition pathway, yielded an activation barrier $\Delta G^{\dagger}$ = 33.0 ± 0.2 kcal mol^{-1} at 150 °C, comparable to that seen for phosphines [1]. A variety of acidic and radical reagents failed to induce any epimerization, although decomposition did occur. Even if one were to worry that such a reagent might nevertheless exist and be responsible for our observed epimerization, the results obtained here clearly establish a lower limit for phosphite inversion. In fact, we would argue that the simplest mechanism is indeed inversion, and that all previous reports of epimerization of cyclic phosphites and related species at low temperature are not due to inversion. While the use of such cyclic phosphites as ligands for catalytic asymmetric reactions is therefore problematic, the use of acyclic P-stereogenic phosphites, which we have shown here to be comparable to phosphines in configurational stability, should now be considered.

4. Experimental

4.1. Materials and methods

NMR spectra were recorded on a 400 MHz Bruker spectrometer with tetramethylsilane and 85% H_3PO_4 in CD_3CN and $CDCl_3$ as external standards. High-resolution mass spectrometry was performed on an Agilent G6520A Q-TOF instrument. Air and water-sensitive compounds were handled in an inert-atmosphere glove box under nitrogen. Amines (except DABCO and dimethyl(cyanomethyl)amine), acetonitrile, and DMF were distilled from calcium hydride under nitrogen, and diethyl ether and THF were distilled from sodium-benzophenone under nitrogen. All other reagents and solvents (including 1,4-diazabicyclo[2.2.2]octane (DABCO) and dimethyl(cyanomethyl)amine) were used as received. Flash column chromatography was carried out on 230–400 mesh silica gel, and TLC was carried out on aluminum-backed silica gel F (200 μm). Starting materials for the synthesis of **15** [33,38] were synthesized according to literature procedures, including $NCCH_2CH_2OPCl_2$ [47], 5′-*O*-(4,4′-dimethoxytrityl)thymidine [34], 2-cyanoethyl 5′-*O*-(4,4′-dimethoxytrityl)-thymidin-3′-yl *N*,*N*-diisopropylphosphoramidite (**8**, Scheme 1) [37,47], and 3′-*O*-(*tert*-butyldimethylsilyl)thymidine [35,36].

For the peak assignments in the ^{1}H NMR spectra of **15**–**18** and **20** that follow, the 3′-phosphorylated thymidine and the

5′-phosphorylated thymidine are labeled T1 and T2, respectively. Peak assignments for **17** and S_P-**18** were determined by 2D COSY, as was differentiation of T1 and T2, which was made possible by coupling of the 5′-hydroxyl hydrogen to the neighboring CH_2 to give a triplet for the hydroxyl hydrogen, with the resulting assignment along with the rest of the coupled hydrogen atoms in that fragment to T1. Peak assignments for S_P-**15**, **16**, R_P-**18**, and **20** were determined by 2D COSY, and differentiation of T1 and T2 was accomplished by comparison of chemical shifts of the two thymidine moieties to those of 5′-*O*-(4,4′-dimethoxytrityl)thymidine and 3′-*O*-(*tert*-butyldimethylsilyl)thymidine.

4.2. Synthesis of pyridinum trifluoroacetate (PTFA)

Trifluoroacetic acid (7.10 g, 62.3 mmol) was added slowly to a vigorously stirred solution of pyridine (4.90 g, 61.9 mmol) in 75 mL of ether. After ~10 min the precipitate was filtered and dried on a vacuum line to give PTFA (10.6 g, 88% yield) as white crystals. ^{1}H NMR (400 MHz, CD_3CN): δ 8.86–7.91 (m, 5H), NH^+ not observed. ^{13}C NMR (100 MHz, CD_3CN): δ 162.1 (q, J = 35.0 Hz), 145.7, 143.8, 127.8, 117.9 (q, J = 292.0 Hz).

4.3. Synthesis of 2-cyanoethyl 5′-O-(4,4′-dimethoxytrityl)thymidin-3′-yl 3′-O-(tert-butyldimethylsilyl)thymidin-5′-yl phosphite (S_P-**15** and R_P-**15**)

In the glove box, a solution of S_P-**16** (0.31 g, 0.31 mmol) and DABCO (0.35 g, 3.10 mmol) in 15 mL of CH_2Cl_2 was stirred for 37 h at rt. The solvent was evaporated on a vacuum line to give crude S_P-**15** as a gum. The gum was applied to a short column of silica gel (~30 g in a coarse frit), and then eluted with THF. All UV-active material moving with the solvent front was collected and the solvent evaporated on a vacuum line to afford S_P-**15** as a white foam (0.184 g, 60% yield). ^{1}H NMR (400 MHz, $CDCl_3$, peaks assigned by 2D COSY): δ 8.42 (br s, NH, 2H), 7.57 (d, J = 1.2 Hz, H-6, 1H), 7.39–6.83 (m, 14H), 6.38 (dd, J = 5.6 Hz, 8.0 Hz, ^{T1}H-1′, 1H), 6.20 (t, J = 6.6 Hz, ^{T2}H-1′, 1H), 4.92 (m, ^{T1}H-3′, 1H), 4.37 (m, ^{T2}H-3′, 1H), 4.15 (m, ^{T1}H-4′, 1H), 4.06–3.88 (m, ^{T2}H-4′, ^{T2}H-5′, ^{T2}H-5″, $NCCH_2CH_2OP$, 5H), 3.79 (s, 2 × CH_3O, 6H), 3.45 (m, ^{T1}H-5′, ^{T1}H-5″, 2H), 2.55 (t, J = 6.0 Hz, CH_2CN, 2H), 2.51–2.12 (m, ^{T1}H-2′, ^{T1}H-2″, ^{T2}H-2′, ^{T2}H-2″, 4H), 1.89 (d, J = 1.2 Hz, CH_3C-5, 3H), 1.45 (d, J = 1.2 Hz, CH_3C-5, 3H), 0.89 (s, $(CH_3)_3$CSi, 9H), 0.083 (s, CH_3Si, 3H), 0.079 (s, CH_3Si, 3H). ^{31}P NMR (161 Mz, $CDCl_3$): δ 140.06.

R_P-***15*** (0.17 g, 65% yield from R_P-**16**): ^{1}H NMR (400 MHz, $CDCl_3$): δ 8.78 (br s, NH, 1H), 8.72 (br s, NH, 1H), 7.57 (d, J = 1.2 Hz, H-6, 1H), 7.39–6.83 (m, 14H), 6.41 (dd, J = 5.6 Hz, 8.1 Hz, ^{T1}H-1′, 1H), 6.19 (t, J = 6.6 Hz, ^{T2}H-1′, 1H), 4.99 (m, ^{T1}H-3′, 1H), 4.33 (m, ^{T2}H-3′, 1H), 4.15 (m, ^{T1}H-4′, 1H), 4.05–3.92 (m, ^{T2}H-4′, ^{T2}H-5′, ^{T2}H-5″, $NCCH_2CH_2OP$, 5H), 3.79 (s, 2 × CH_3O, 6H), 3.41 (m, ^{T1}H-5′, ^{T1}H-5″, 2H), 2.60 (t, J = 6.0 Hz, CH_2CN, 2H), 2.54–2.11 (m, ^{T1}H-2′, ^{T1}H-2″, ^{T2}H-2′, ^{T2}H-2″, 4H), 1.89 (d, J = 1.2 Hz, CH_3C-5, 3H), 1.45 (d, J = 1.2 Hz, CH_3C-5, 3H), 0.87 (s, $(CH_3)_3$CSi, 9H), 0.062 (s, CH_3Si, 3H), 0.057 (s, CH_3Si, 3H). ^{31}P NMR (161 Mz, $CDCl_3$): δ 139.87.

4.4. Synthesis and separation of 2-cyanoethyl 5′-O-(4,4′-dimethoxytrityl)thymidin-3′-yl 3′-O-(tert-butyldimethylsilyl)thymidin-5′-yl boranophosphate (S_P-**16** and R_P-**16**)

Details of the synthesis of **16** and NMR spectra have not been reported [33,38]. Under nitrogen, PTFA (0.8524 g, 4.414 mmol) and *N*-methylimidazole (NMI) (0.1919 g, 2.337 mmol) were dissolved in 8 mL CH_3CN and then added dropwise over ~5 min to a magnetically stirred solution of **8** (1.6514 g, 2.2172 mmol) and 3′-*O*-(*tert*-butyldimethylsilyl)thymidine (0.7191 g, 2.017 mmol) dissolved in 20 mL CH_3CN. After 1 h, the reaction solution was evaporated on a vacuum line to give a gum. The gum was dissolved in 60 mL CH_2Cl_2 and then washed with 20 mL saturated Na_2CO_3 solution. The organic layer was dried with anhydrous $MgSO_4$, and the solvent evaporated on a vacuum line to give a foam. The foam was dissolved in 25 mL dry THF and the solution placed under N_2 in an ice-water bath. To the stirred solution, $Me_2S{\cdot}BH_3$ (3.4 mL of a 2.0 M solution in THF, 6.8 mmol) was added dropwise over ~3–4 min. The ice-water bath was removed after addition of the $Me_2S{\cdot}BH_3$ solution and the solution was allowed to stir for an additional 10 min, after which it was immediately eluted through a pad of silica gel (~100 g in a 150 mL coarse frit) with THF. All the UV active material moving with the solvent front was collected and the solvent was evaporated on a vacuum line to give crude **16** as a white foam (1.94 g, 95%). The two diastereomers of **16** were separated by silica gel chromatography using 4:1 EtOAc/hexanes (120 g silica gel in a 30 mm diameter column). The fractions corresponding to R_f = 0.56 and 0.44 were combined separately and evaporated on a vacuum line to give white foams. The ^{1}H NMR spectra of both samples showed that N-methylimidazole was present, so each sample was dissolved in 50 mL EtOAc/hexanes (2/1) and then washed with 25 mL of 0.5 M citric acid. The organic layer was dried with $MgSO_4$ and then evaporated on a vacuum line to afford S_P-**16** (0.49 g, 25% yield) and R_P-**16** (0.44 g, 23% yield) as white foams. S_P-**16** (R_f = 0.56, in 4:1 EtOAc/hexanes): ^{1}H NMR (400 MHz, CD_3CN, peaks assigned by 2D COSY): δ 9.36 (br s, NH, 2H), 7.44–7.24 (m, ArH, 2 × H-6, 11H), 6.88–6.86 (m, ArH, 4H), 6.28 (dd, J = 5.9, 8.3 Hz, ^{T1}H-1′, 1H), 6.14 (t, J = 6.8 Hz, ^{T2}H-1′, 1H), 5.20 (m, ^{T1}H-3′, 1H), 4.41 (m, ^{T2}H-3′, 1H), 4.26–4.13 (m, ^{T1}H-4′, ^{T2}H-5′, ^{T2}H-5″, $NCCH_2CH_2OP$, 5H), 3.94 (m, ^{T2}H-4′, 1H), 3.76 (s, CH_3O, 6H), 3.33 (m, ^{T1}H-5′, ^{T1}H-5″, 2H), 2.72 (t, J = 5.9 Hz, CH_2CN, 2H), 2.48 (m, ^{T1}H-2′, ^{T1}H-2″, 2H), 2.18 (m, ^{T2}H-2′, ^{T2}H-2″, 2H), 1.82 (s, CH_3C-5, 3H), 1.45 (s, CH_3C-5, 3H), 0.89 (s, $(CH_3)_3$CSi, 9H), 0.45 (br, BH_3, 3H), 0.099 (s, CH_3Si, 3H), 0.096 (s, CH_3Si, 3H). ^{13}C NMR (100 MHz, CD_3CN): δ 164.7, 159.9, 151.5, 151.4, 145.7, 137.0, 136.6, 136.39, 136.37, 131.1, 131.0, 129.03, 128.98, 128.1, 114.2, 111.8, 111.6, 87.8, 85.7, 85.5 (d, J = 6.5 Hz), 85.31 (d, J = 5.1 Hz), 85.28, 79.4 (d, J = 1.7 Hz), 72.4, 67.0 (d, J = 5.0 Hz), 64.2, 62.9 (d, J = 3.0 Hz), 56.0, 40.4, 39.6 (d, J = 3.0 Hz), 26.1, 20.3 (d, J = 6.5 Hz), 18.6, 12.7, 12.2, −4.5, −4.6; the peak for the CN group is presumed to be hidden under the solvent peak of CD_3CN at 118.3 ppm. ^{31}P NMR (161 Mz, CD_3CN): δ 116.89. HRMS (ESI): Calcd for $C_{50}H_{64}BN_5O_{13}PSi$ $[M-H]^-$: 1012.4101, found 1012.4100.

R_P-***16*** (R_f = 0.44, in 4:1 EtOAc/hexanes): ^{1}H NMR (400 MHz, CD_3CN, peaks assigned by 2D COSY): δ 9.31 (br s, NH, 1H), 9.28 (br s, NH, 1H), 7.44–7.21 (m, ArH, 2 × H-6, 11H), 6.88–6.85 (m, ArH, 4H), 6.28 (dd, J = 6.1, 8.1 Hz, ^{T1}H-1′, 1H), 6.12 (t, J = 6.8 Hz, ^{T2}H-1′, 1H), 5.21 (m, ^{T1}H-3′, 1H), 4.38 (m, ^{T2}H-3′, 1H), 4.20–4.16 (m, ^{T1}H-4′, ^{T2}H-5′, ^{T2}H-5″, $NCCH_2CH_2OP$, 5H), 3.93 (m, ^{T2}H-4′, 1H), 3.75 (s, CH_3O, 6H), 3.32 (m, ^{T1}H-5′, ^{T1}H-5″, 2H), 2.74 (t, J = 5.8 Hz, CH_2CN, 2H), 2.50 (m, ^{T1}H-2′, ^{T1}H-2″, 2H), 2.18 (m, ^{T2}H-2′, ^{T2}H-2″, 2H), 1.80 (s, CH_3C-5, 3H), 1.45 (s, CH_3C-5, 3H), 0.88 (s, $(CH_3)_3$CSi, 9H), 0.44 (br, BH_3, 3H), 0.077 (s, $(CH_3)_2$Si, 6H). ^{13}C NMR (100 MHz, CD_3CN): δ 164.71, 164.66, 159.8, 151.5, 151.4, 145.7, 137.0, 136.6, 136.41, 136.36, 131.07, 131.03, 129.02, 128.97, 128.0, 114.2, 111.7, 111.5, 87.8, 86.0, 85.6 (d, J = 6.6 Hz), 85.30 (d, J = 5.1 Hz), 85.33, 79.3 (d, J = 1.7 Hz), 72.6, 67.3 (d, J = 5.0 Hz), 64.2, 63.0 (d, J = 2.8 Hz), 56.0, 40.4, 39.6 (d, J = 3.3 Hz), 26.1, 20.4 (d, J = 6.5 Hz), 18.5, 12.6, 12.2, −4.5, −4.6; the peak for the CN group is presumed to be under the solvent peak of CD_3CN at 118.3 ppm. ^{31}P NMR (161 Mz, CD_3CN): δ 116.83. HRMS (ESI): Calcd for $C_{50}H_{64}BN_5O_{13}PSi$ $[M-H]^-$: 1012.4101, found 1012.4104.

4.5. Synthesis of 2-cyanoethyl thymidin-3′-yl 3′-O-(tert-butyldimethylsilyl)thymidin-5′-yl boranophosphate (S_P-**17** and R_P-**17**)

A cooled solution of 2% $CHCl_2COOH/CH_2Cl_2$ (15 mL) was added to S_P-**16** (0.32 g, 0.32 mmol) and stirred for 20 min at rt. The

reaction solution was then diluted further with 15 mL CH_2Cl_2 and washed with 5% $NaHCO_3$ (10 mL). The organic layer was removed and the aqueous layer washed with 3 × 10 mL CH_2Cl_2. The combined organic layers were dried with anhydrous $MgSO_4$, filtered, and evaporated on a vacuum line to give a gum. The crude material was dissolved in EtOAc/hexanes (2:1) and applied to a short column of silica gel (~30 g in a 20 mm diameter column). The material was first eluted with 2:1 EtOAc/hexanes, then 4:1 EtOAc/hexanes, and finally with EtOAc. The appropriate fractions with R_f = 0.5 (EtOAc) were pooled, and the solvent was evaporated on a vacuum line to afford S_P-**17** as a white foam (0.18 g, 82% yield). ^{1}H NMR (400 MHz, CD_3CN, peaks assigned by 2D COSY): δ 9.23 (br s, NH, 2H), 7.53 (d, J = 1.2 Hz, H-6, 1H), 7.27 (d, J = 1.2 Hz, H-6, 1H), 6.20 (m, ^{T1}H-1′, ^{T2}H-1′, 2H), 5.06 (m, ^{T1}H-3′, 1H), 4.44 (m, ^{T2}H-3′, 1H), 4.29–4.18 (m, ^{T2}H-5′, ^{T2}H-5″, NCCH$_2$C*H*$_2$OP, 4H), 4.14 (m, ^{T1}H-4′, 1H), 3.98 (m, ^{T2}H-4′, 1H), 3.71 (m, ^{T1}H-5′, ^{T1}H-5″, 2H), 3.33 (br t, J = 5.1 Hz, ^{T1}O*H*), 2.79 (t, J = 5.9 Hz, C*H*$_2$CN, 2H), 2.38 (m, ^{T1}H-2′, ^{T1}H-2″, 2H), 2.21 (m, ^{T2}H-2′, ^{T2}H-2″, 2H), 1.85 (d, J = 1.2 Hz, C*H*$_3$C-5, 3H), 1.82 (d, J = 1.2 Hz, C*H*$_3$C-5, 3H), 0.90 (s, (C*H*$_3$)$_3$CSi, 9H), 0.46 (br, B*H*$_3$, 3H), 0.110 (s, C*H*$_3$Si, 3H), 0.105 (s, C*H*$_3$Si, 3H). ^{13}C NMR (100 MHz, CD_3CN): δ 164.7, 151.54, 151.46, 137.0, 136.9, 118.5, 111.6, 111.5, 86.5 (d, J = 4.4 Hz), 85.8, 85.7, 85.5 (d, J = 6.6 Hz), 79.4 (d, J = 2.2 Hz), 72.4, 67.0 (d, J = 4.8 Hz), 62.9 (d, J = 3.3 Hz), 62.3, 40.3, 39.3 (d, J = 3.0 Hz), 26.1, 20.4 (d, J = 6.5 Hz), 18.6, 12.7, 12.6, −4.5, −4.7. ^{31}P NMR (161 Mz, CD_3CN): δ 116.47. HRMS (ESI): Calcd for $C_{29}H_{48}BN_5O_{11}PSi$ $[M+H]^+$: 712.2950, found 712.2962.

R_P-***17*** (0.12 g, 87% yield from R_P-**16**): ^{1}H NMR (400 MHz, CD_3CN, peaks assigned by 2D COSY): δ 9.27 (br s, NH, 1H), 9.26 (br s, NH, 1H), 7.54 (d, J = 1.2 Hz, H-6, 1H), 7.27 (d, J = 1.2 Hz, H-6, 1H), 6.20 (m, ^{T1}H-1′, ^{T2}H-1′, 2H), 5.08 (m, ^{T1}H-3′, 1H), 4.43 (m, ^{T2}H-3′, 1H), 4.27–4.17 (m, ^{T2}H-5′, ^{T2}H-5″, NCCH$_2$C*H*$_2$OP, 4H), 4.13 (m, ^{T1}H-4′, 1H), 3.98 (m, ^{T2}H-4′, 1H), 3.71 (m, ^{T1}H-5′, ^{T1}H-5″, 2H), 3.35 (br t, J = 5.1 Hz, ^{T1}O*H*), 2.79 (t, J = 5.9 Hz, C*H*$_2$CN, 2H), 2.38 (m, ^{T1}H-2′, ^{T1}H-2″, 2H), 2.20 (m, ^{T2}H-2′, ^{T2}H-2″, 2H), 1.85 (d, J = 1.2 Hz, C*H*$_3$C-5, 3H), 1.82 (d, J = 1.2 Hz, C*H*$_3$C-5, 3H), 0.90 (s, (C*H*$_3$)$_3$CSi, 9H), 0.49 (br, B*H*$_3$, 3H), 0.111 (s, C*H*$_3$Si, 3H), 0.104 (s, C*H*$_3$Si, 3H). ^{13}C NMR (100 MHz, CD_3CN): δ 164.74, 164.71, 151.6, 151.5, 137.1, 137.0, 118.5, 111.6, 111.5, 86.5 (d, J = 4.4 Hz), 85.8, 85.7, 85.5 (d, J = 6.3 Hz), 79.2 (d, J = 3.6 Hz), 72.5, 67.1 (d, J = 4.4 Hz), 63.1 (d, J = 2.9 Hz), 62.3, 40.4, 39.3 (d, J = 3.0 Hz), 26.1, 20.4 (d, J = 6.5 Hz), 18.6, 12.64, 12.62, −4.5, −4.7. ^{31}P NMR (161 Mz, CD_3CN): δ 116.25. HRMS (ESI): Calcd for $C_{29}H_{48}BN_5O_{11}PSi$ $[M+H]^+$: 712.2950, found 712.2957.

*4.6. Synthesis of 2-cyanoethyl thymidin-3′-yl thymidin-5′-yl boranophosphate (S_P-**18** and R_P-**18**)*

Compound S_P-**17** (0.17 g, 0.24 mmol) was dissolved in 8 mL THF and HF pyridine (0.54 mL, 5.99 mmol) was added to the magnetically stirred solution. After ~20 h at rt, TLC indicated complete conversion to the product. The reaction solution was evaporated on a vacuum line to dryness, then redissolved in 10 mL MeOH and evaporated on 1 g silica gel. The material was applied to a silica gel column (~20 g in a 20 mm diameter column) and eluted with 10% MeOH/EtOAc. The appropriate fractions with R_f = 0.42 (10% MeOH/EtOAc) were combined and the solvent evaporated on a vacuum line to afford S_P-**18** as a white foam (0.123 g, 87% yield). ^{1}H NMR (400 MHz, CD_3CN, peaks assigned by 2D COSY): δ 9.27 (br s, NH, 2H), 7.54 (d, J = 1.2 Hz, H-6, 1H), 7.28 (d, J = 1.2 Hz, H-6, 1H), 6.21 (m, ^{T1}H-1′, ^{T2}H-1′, 2H), 5.07 (m, ^{T1}H-3′, 1H), 4.36 (m, ^{T2}H-3′, 1H), 4.31–4.20 (m, ^{T2}H-5′, ^{T2}H-5″, NCCH$_2$C*H*$_2$OP, 4H), 4.14 (m, ^{T1}H-4′, 1H), 3.99 (m, ^{T2}H-4′, 1H), 3.71 (m, ^{T1}H-5′, ^{T1}H-5″, 2H), 3.60 (br s, ^{T2}O*H*), 3.36 (br t, J = 4.7 Hz, ^{T1}O*H*), 2.79 (t, J = 6.0 Hz, C*H*$_2$CN, 2H), 2.37 (m, ^{T1}H-2′, ^{T1}H-2″, 2H), 2.18 (m, ^{T2}H-2′, ^{T2}H-2″, 2H), 1.85 (d, J = 1.2 Hz, C*H*$_3$C-5, 3H), 1.82 (d, J = 1.2 Hz, C*H*$_3$C-5, 3H), 0.46 (br, B*H*$_3$, 3H). ^{13}C NMR (100 MHz, CD_3CN): δ 164.73, 164.71, 151.6, 151.5, 137.1, 136.8, 118.6, 111.64, 111.55, 86.5 (d, J = 4.6 Hz), 85.8, 85.5, 85.2 (d, J = 6.6 Hz), 79.4 (d, J = 2.6 Hz), 71.3, 67.3 (d, J = 4.8 Hz), 62.9 (d, J = 3.0 Hz), 62.3, 39.9, 39.3 (d, J = 3.0 Hz), 20.4 (d, J = 6.7 Hz), 12.7, 12.6. ^{31}P NMR (161 Mz, CD_3CN): δ 116.21. HRMS (ESI): Calcd for $C_{23}H_{34}BN_5O_{11}P$ $[M+H]^+$: 598.2086, found 598.2095.

R_P-***18*** (78 mg, 85% yield from R_P-**17**): ^{1}H NMR (400 MHz, CD_3CN, peaks assigned by 2D COSY): δ 9.19 (br s, NH, 2H), 7.53 (d, J = 1.2 Hz, H-6, 1H), 7.28 (d, J = 1.2 Hz, H-6, 1H), 6.20 (m, ^{T1}H-1′, ^{T2}H-1′, 2H), 5.08 (m, ^{T1}H-3′, 1H), 4.35 (m, ^{T2}H-3′, 1H), 4.30–420 (m, ^{T2}H-5′, ^{T2}H-5″, NCCH$_2$C*H*$_2$OP, 4H), 4.14 (m, ^{T1}H-4′, 1H), 3.99 (m, ^{T2}H-4′, 1H), 3.72 (m, ^{T1}H-5′, ^{T1}H-5″, 2H), 3.56 (br s, ^{T2}O*H*), 3.36 (br s, ^{T1}O*H*), 2.79 (t, J = 6.0 Hz, C*H*$_2$CN, 2H), 2.39 (m, ^{T1}H-2′, ^{T1}H-2″, 2H), 2.20 (m, ^{T2}H-2′, ^{T2}H-2″, 2H), 1.85 (d, J = 1.2 Hz, C*H*$_3$C-5, 3H), 1.83 (d, J = 1.2 Hz, C*H*$_3$C-5, 3H), 0.46 (br, B*H*$_3$, 3H). ^{13}C NMR (100 MHz, CD_3CN): δ 164.70, 164.67, 151.6, 151.5, 137.1, 136.8, 118.5, 111.6, 111.5, 86.50 (d, J = 4.5 Hz), 85.9, 85.6, 85.3 (d, J = 6.6 Hz), 79.3 (d, J = 3.2 Hz), 71.4, 67.4 (d, J = 4.8 Hz), 63.0 (d, J = 3.0 Hz), 62.3, 39.9, 39.2 (d, J = 2.9 Hz), 20.4 (d, J = 6.7 Hz), 12.65, 12.60. ^{31}P NMR (161 Mz, CD_3CN): δ 115.90. HRMS (ESI): Calcd for $C_{23}H_{34}BN_5O_{11}P$ $[M+H]^+$: 598.2086, found 598.2099.

*4.7. Synthesis of 2-cyanoethyl thymidin-3′-yl thymidin-5′-yl phosphite (S_P-**19** and R_P-**19**)*

In the glove box, a solution of S_P-**18** (0.115 g, 0.192 mmol) in 2 mL of pyridine was stirred for 36 h at rt. The solution was then evaporated over 1 g of silica gel on a vacuum line. The material was applied to a short column of silica gel (~10 g in a coarse frit) and then eluted with 5% MeOH/EtOAc followed by 5% MeOH/THF. All fractions with R_f = 0.54 (5% MeOH/THF) were combined and the solvent evaporated on a vacuum line to afford S_P-**19** as a white foam (0.10 g, 90% yield). ^{1}H NMR (400 MHz, CD_3CN): δ 9.04 (br s, NH, 2H), 7.53 (d, J = 1.2 Hz, H-6, 1H), 7.40 (d, J = 1.2 Hz, H-6, 1H), 6.22–6.16 (m, H-1′, 2H), 4.87 (m, H-3′, 1H), 4.35 (m, H-3′, 1H), 4.09–4.00 (m, H-5′ (2H), H-4′ (1H), NCCH$_2$C*H*$_2$OP, 5H), 3.95 (m, H-4′, 1H), 3.70 (m, H-5′, 2H), 3.50 (br s, O*H*, 1H), 3.27 (br s, O*H*, 1H), 2.70 (t, J = 5.9 Hz, C*H*$_2$CN, 2H), 2.37–2.23 (m, H-2′, 2H), 2.20–2.14 (m, H-2′, 2H), 1.84 (d, J = 1.2 Hz, C*H*$_3$-C-5, 3H), 1.82 (d, J = 1.2 Hz, C*H*$_3$-C-5, 3H). ^{31}P NMR (161 Mz, CD_3CN): δ 140.78.

R_P-***19*** (90 mg, 80% yield from R_P-**18**): ^{1}H NMR (400 MHz, CD_3CN): δ 9.03 (br s, NH, 2H), 7.53 (s, H-6, 1H), 7.39 (s, H-6, 1H), 6.21–6.17 (m, H-1′, 2H), 4.91 (m, H-3′, 1H), 4.34 (m, H-3′, 1H), 4.04–4.01 (m, H-5′ (2H), H-4′ (1H), NCCH$_2$C*H*$_2$OP, 5H), 3.94 (m, H-4′, 1H), 3.71 (m, H-5′, 2H), 3.48 (br s, O*H*, 1H), 3.26 (br s, O*H*, 1H), 2.70 (t, J = 5.9 Hz, C*H*$_2$CN, 2H), 2.37–2.26 (m, H-2′, 2H), 2.19–2.14 (m, H-2′, 2H), 1.84 (s, C*H*$_3$-C-5, 3H), 1.82 (s, C*H*$_3$-C-5, 3H). ^{31}P NMR (161 Mz, CD_3CN): δ 140.37.

*4.8. Synthesis of 2-cyanoethyl 5′-O-(acetyl)thymidin-3′-yl 3′-O-(acetyl)thymidin-5′-yl phosphite (S_P-**20** and R_P-**20**)*

In the glove box, a solution of S_P-**18** (80.3 mg, 0.138 mmol) and acetic anhydride (2.089 mg, 0.2133 mmol) in 4 mL of pyridine, was stirred for 24 h at rt. Approximately 0.5 g silica gel was then added to the flask and then the excess pyridine was evaporated on a vacuum line. The silica gel containing the crude product was applied to a short column of silica gel (~10 g in a 15 mL coarse frit), then eluted with EtOAc followed by 2:1 EtOAc/THF and then THF. The fractions with R_f = 0.41 (2:1 EtOAc/THF) were combined and the solvent evaporated on a vacuum line to afford S_P-**20** as a white foam (76.3 mg, 83% yield). ^{1}H NMR (400 MHz, CD_3CN, peaks assigned by 2D COSY): δ 9.30 (br s, NH, 2H), 7.42 (d, J = 1.2 Hz, H-6,

1H), 7.30 (d, J = 1.2 Hz, H-6, 1H), 6.20 (m, ^{T1}H-1′, ^{T2}H-1′, 2H), 5.23 (m, ^{T1}H-3′, 1H), 4.84 (m, ^{T2}H-3′, 1H), 4.25–4.02 (m, ^{T2}H-5′, ^{T2}H-5″, ^{T1}H-5′, ^{T1}H-5″, ^{T1}H-4′, ^{T2}H-4′, NCCH$_2$CH_2OP, 8H), 2.71 (t, J = 5.9 Hz, CH_2CN, 2H), 2.42–2.25 (m, ^{T1}H-2′, ^{T1}H-2″, ^{T2}H-2′, ^{T2}H-2″, 4H), 2.043 (s, CH_3), 2.040 (s, CH_3), 1.84 (d, J = 1.2 Hz, CH_3C-5, 3H), 1.83 (d, J = 1.2 Hz, CH_3C-5, 3H). ^{13}C NMR (100 MHz, CD$_3$CN): δ 171.41, 171.36, 164.7 (br s), 151.5, 151.4, 136.65, 135.61, 119.3, 111.7, 111.5, 85.7, 85.5, 84.1 (d, J = 5.5 Hz), 84.0 (d, J = 3.9 Hz), 74.9, 73.9 (d, J = 13.9 Hz), 64.2, 63.5 (d, J = 9.1 Hz), 58.7 (d, J = 9.8 Hz), 39.5 (br s), 37.4, 21.2, 21.1, 20.9 (d, J = 4.5 Hz), 12.7, 12.6. ^{31}P NMR (161 Mz, CD$_3$CN): δ 140.78. HRMS (ESI): Calcd for $C_{27}H_{33}N_5O_{13}P$ [M−H]$^-$: 666.1813, found 666.1828.

R_P-***20*** (67 mg, 84% yield from R_P-**18**): ^{1}H NMR (400 MHz, CD$_3$CN, peaks assigned by 2D COSY): δ 9.21 (br s, NH, 2H), 7.40 (d, J = 1.2 Hz, H-6, 1H), 7.31 (d, J = 1.2 Hz, H-6, 1H), 6.20 (m, ^{T1}H-1′, ^{T2}H-1′, 2H), 5.23 (m, ^{T1}H-3′, 1H), 4.89 (m, ^{T2}H-3′, 1H), 4.25–4.00 (m, ^{T2}H-5′, ^{T2}H-5″, ^{T1}H-5′, ^{T1}H-5″, ^{T1}H-4′, ^{T2}H-4′, NCCH$_2$CH_2OP, 8H), 2.70 (t, J = 5.9 Hz, CH_2CN, 2H), 2.42–2.25 (m, ^{T1}H-2′, ^{T1}H-2″, ^{T2}H-2′, ^{T2}H-2″, 4H), 2.044 (s, CH_3), 2.040 (s, CH_3), 1.843 (d, J = 1.2 Hz, CH_3C-5, 3H), 1.836 (d, J = 1.2 Hz, CH_3C-5, 3H). ^{13}C NMR (100 MHz, CD$_3$CN): δ 171.39, 171.37, 164.7 (br s), 151.5, 151.4, 136.63, 136.57, 119.2, 111.6, 111.5, 85.6 (br s), 84.11 (d, J = 5.6 Hz), 84.06 (d, J = 3.5 Hz), 75.0, 73.5 (d, J = 9.9 Hz), 64.2, 63.5 (d, J = 9.1 Hz), 59.1 (d, J = 13.6 Hz), 39.5 (br s), 37.5, 21.2, 21.1, 20.9 (d, J = 4.9 Hz), 12.7, 12.6. ^{31}P NMR (161 Mz, CD$_3$CN): δ 140.32. HRMS (ESI): Calcd for $C_{27}H_{33}N_5O_{13}P$ [M−H]$^-$: 666.1813, found 666.1831.

4.9. NMR experiments

In the glove box, samples of S_P-**15**, S_P-**19**, and S_P- and R_P-**20** were weighed and dissolved in ~0.5 mL of toluene-d_8 (for **15**) or CD$_3$CN (for **19** and **20**), and placed in an NMR tube sealed to a 14/20 joint. For **15** and **19**, no reference standards were used. For **20**, PPh$_3$ was added to two samples (internal standards) while for the other samples, a solution of PPh$_3$ in CH$_3$CN was prepared and added to melting point capillaries that were then sealed with a microburner, and the sealed capillaries were added to the NMR tubes (external standards). For two of the experiments, both the NMR tubes and capillary tubes were silanized [39]. Following sample preparation in the glove box, a vacuum stopcock was attached to each NMR tube, which was then removed from the glove box. The tubes were each attached to a vacuum line, nitrogen was removed by three freeze–pump–thaw cycles, and they were then sealed with a torch. For kinetics experiments, the tubes were heated in a thermostatted oil bath at 150.0 ± 0.2 °C with approximately 1 in. of the inverted tube above the level of the oil. The tubes were taken out every 30 min and immediately submerged in a water bath kept at ~20 °C for ~5 min, and then the ^{31}P NMR spectra were recorded. All sample data for **20** (including concentrations at each time point for the six experiments) may be found in Supplementary material.

Acknowledgment

We thank Queens College and the City University of New York PSC-CUNY Research Award Program for financial support.

Appendix A. Supplementary material

NMR spectra of dinucleosides including selected ^{31}P NMR spectra of epimerization experiments, kinetic data and plots of the best-fit lines for the decomposition and epimerization of **20**, experimental procedures and table of results for Section 2.7, and spectra of acids used. Supplementary data associated with this article can be found, in the online version, at doi:10.1016/j.ica.2010.11.022.

References

[1] R.D. Baechler, K. Mislow, J. Am. Chem. Soc. 92 (1970) 3090.
[2] M. Mizuguchi, K. Makino, Nucleosides Nucleotides 15 (1996) 407.
[3] A.J. Minnaard, B.L. Feringa, L. Lefort, J.G. de Vries, Acc. Chem. Res. 40 (2007) 1267.
[4] M.T. Reetz, H. Guo, J.-A. Ma, R. Goddard, R.J. Mynott, J. Am. Chem. Soc. 131 (2009) 4136.
[5] J. Mazuela, J.J. Verendel, M. Coll, B. Schäffner, A. Börner, P.G. Andersson, O. Pàmies, M. Diéguez, J. Am. Chem. Soc. 131 (2009) 12344.
[6] K. Nozaki, N. Sakai, T. Nanno, T. Higashijima, S. Mano, T. Horiuchi, H. Takaya, J. Am. Chem. Soc. 119 (1997) 4413.
[7] C.J. Cobley, K. Gardner, J. Klosin, C. Praquin, C. Hill, G.T. Whiteker, A. Zanotti-Gerosa, J.L. Petersen, K.A. Abboud, J. Org. Chem. 69 (2004) 4031.
[8] Y. Yan, X. Zhang, J. Am. Chem. Soc. 128 (2006) 7198.
[9] C.J. Cobley, R.D.J. Froese, J. Klosin, C. Qin, G.T. Whiteker, K.A. Abboud, Organometallics 26 (2007) 2986.
[10] Y. Zou, Y. Yan, X. Zhang, Tetrahedron Lett. 48 (2007) 4781.
[11] T. Robert, Z. Abiri, J. Wassenaar, A.J. Sandee, S. Romanski, J.-M. Neudörfl, H.-G. Schmalz, J.N.H. Reek, Organometallics 29 (2010) 478.
[12] Y. Jin, G. Biancotto, G. Just, Tetrahedron Lett. 37 (1996) 973.
[13] J.-C. Wang, G. Just, J. Org. Chem. 64 (1999) 8090.
[14] R.P. Iyer, D. Yu, N.-H. Ho, W. Tan, S. Agrawal, Tetrahedron Asymmetr. 6 (1995) 1051.
[15] R.P. Iyer, M.-J. Guo, D. Yu, S. Agrawal, Tetrahedron Lett. 39 (1998) 2491.
[16] D. Yu, E.R. Kandimalla, A. Roskey, Q. Zhao, L. Chen, J. Chen, S. Agrawal, Bioorg. Med. Chem. 8 (2000) 275.
[17] A. Wilk, A. Grajkowski, L.R. Phillips, S.L. Beaucage, J. Am. Chem. Soc. 122 (2000) 2149.
[18] N. Oka, T. Wada, K. Saigo, J. Am. Chem. Soc. 125 (2003) 8307.
[19] N. Oka, M. Yamamoto, T. Sato, T. Wada, J. Am. Chem. Soc. 130 (2008) 16031.
[20] N. Oka, T. Kondo, S. Fujiwara, Y. Maizuru, T. Wada, Org. Lett. 11 (2009) 967.
[21] Z. Xin, G. Just, Tetrahedron Lett. 37 (1996) 969.
[22] M. Fujii, K. Ozaki, A. Kume, M. Sekine, T. Hata, Tetrahedron Lett. 27 (1986) 3365.
[23] M. Fujii, K. Ozaki, M. Sekine, T. Hata, Tetrahedron 43 (1987) 3395.
[24] M. Mizuguchi, K. Makino, Patent Written in Japanese, JP 08245665, 1996, 10pp.
[25] W.G. Bentrude, A.E. Sopchik, T. Gajda, J. Am. Chem. Soc. 111 (1989) 3981.
[26] Y. Hayakawa, Y. Hirabayashi, M. Hyodo, S. Yamashita, T. Matsunami, D.-M. Cui, R. Kawai, H. Kodama, Eur. J. Org. Chem. (2006) 3834–3844.
[27] Y. Huang, J. Yu, W.G. Bentrude, J. Org. Chem. 60 (1995) 4767.
[28] H. Hommer, B. Gordillo, Phosphorus, Sulfur Silicon 177 (2002) 465.
[29] S. Jugé, M. Stephan, J.A. Laffitte, J.P. Genet, Tetrahedron Lett. 31 (1990) 6357.
[30] J.M. Brown, J.V. Carey, M.J.H. Russell, Tetrahedron 46 (1990) 4877.
[31] T. Johansson, J. Stawinski, Bioorg. Med. Chem. 9 (2001) 2315.
[32] P. Heinonen, A. Winqvist, Y. Sanghvi, R. Strömberg, Nucleosides, Nucleotides Nucleic Acids 22 (2003) 1387.
[33] Y. Jin, G. Just, Tetrahedron Lett. 39 (1998) 6429.
[34] H. Schaller, G. Weimann, B. Lerch, H.G. Khorana, J. Am. Chem. Soc. 85 (1963) 3821.
[35] K.K. Ogilvie, Can. J. Chem. 51 (1973) 3799.
[36] K.K. Ogilvie, E.A. Thompson, M.A. Quilliam, J.B. Westmore, Tetrahedron Lett. (1974) 2865–2868.
[37] Y. Hayakawa, M. Kataoka, J. Am. Chem. Soc. 120 (1998) 12395.
[38] A. Eleuteri, D.C. Capaldi, A.H. Krotz, D.L. Cole, V.T. Ravikumar, Org. Process Res. Dev. 4 (2000) 182.
[39] R.P. Iyer, L.R. Phillips, W. Egan, J.B. Regan, S.L. Beaucage, J. Org. Chem. 55 (1990) 4693.
[40] W.H. Hersh, R.H. Fong, Organometallics 24 (2005) 4179.
[41] E. Vedejs, Y. Donde, J. Org. Chem. 65 (2000) 2337.
[42] S. Humbel, C. Bertrand, C. Darcel, C. Bauduin, S. Jugé, Inorg. Chem. 42 (2003) 420.
[43] W. Perlikowska, M. Gouygou, M. Mikolajczyk, J.-C. Daran, Tetrahedron Asymmetr. 15 (2004) 3519.
[44] S. Berner, K. Mühlegger, H. Seliger, Nucleic Acids Res. 17 (1989) 853.
[45] D.W. Reynolds, K.T. Lorenz, H.-S. Chiou, D.J. Bellville, R.A. Pabon, N.L. Bauld, J. Am. Chem. Soc. 109 (1987) 4960.
[46] Y. Hayakawa, R. Kawai, A. Hirata, J. Sugimoto, M. Kataoka, A. Sakakura, M. Hirose, R. Noyori, J. Am. Chem. Soc. 123 (2001) 8165.
[47] C.A.A. Claesen, R.P.A.M. Segers, G.I. Tesser, Recl. Trav. Chim. Pays-Bas 104 (1985) 119.